

PHOTON-PARTON SPLITTING FUNCTIONS AT
THE NEXT-TO-NEXT-TO-LEADING ORDER OF QCD*

A. VOGT

IPPP, Department of Physics, University of Durham
South Road, Durham DH1 3LE, United Kingdom

S. MOCH

Deutsches Elektronensynchrotron DESY
Platanenallee 6, 15735 Zeuthen, Germany

J. VERMASEREN

NIKHEF Theory Group
Kruislaan 409, 1098 SJ Amsterdam, The Netherlands*(Received December 9, 2005)*

We have calculated the splitting functions governing the evolution of the unpolarized parton distributions of the photon at the next-to-next-to-leading order (NNLO) of massless perturbative QCD. The results, presented here mainly in terms of compact and accurate parametrizations, are consistent with our previous approximations based on the lowest six even-integer Mellin moments. Consequently the NNLO corrections are small in both the $\overline{\text{MS}}$ and the DIS_γ factorization schemes at momentum fractions $x \gtrsim 0.1$.

PACS numbers: 12.38.Bx, 13.60.Hb, 13.66.Bc, 14.70.Bh

The partonic structure of the photon, accessed in particular by the deep-inelastic structure function F_2^γ , is a classic subject in perturbative QCD. The leading-order (LO) and next-to-leading order (NLO) expressions for the photon-parton splitting functions $P_{p\gamma}$, $p = q, g$, and the coefficient functions $c_{2,\gamma}$ have been known for a long time [1–6]. A couple of years ago we have presented [7] the corresponding next-to-next-to-leading order (NNLO) corrections, albeit with one important qualification concerning the $\mathcal{O}(\alpha\alpha_s^2)$

* Presented by A. V. at the PHOTON2005 Conference, 31 August–4 September 2005, Warsaw, Poland.

splitting functions: at that time we were only able to derive the lowest six even-integer Mellin moments, $N = 2, \dots, 12$, which are sufficient for a reliable reconstruction only at momentum fractions $x \gtrsim 0.05$.

Using the methods and results derived in the meantime for the hadronic case [8–10], we are now able to present the complete results for the splitting functions and coefficient functions to order $\alpha\alpha_s^2$, thus finalizing the NNLO description and providing an important partial result for F_2^γ at N³LO. In the present brief contribution, we confine ourselves to the NNLO splitting functions, presenting accurate compact parametrizations of those results which are rather lengthy. Furthermore, we take a first look at their numerical effects. A more detailed account, including the exact results and the $\alpha\alpha_s^2$ photonic coefficient functions for F_2 and F_L , will be presented elsewhere [11].

At the lowest order in the electromagnetic coupling $a_{\text{em}} \equiv \alpha_{\text{em}}/(4\pi)$, the parton distributions of the photon are subject to the evolution equations of the form

$$\frac{d\mathbf{q}^\gamma}{d\ln\mu^2} = \mathbf{P}^\gamma + \mathbf{P} \otimes \mathbf{q}^\gamma, \quad (1)$$

where μ represents the $\overline{\text{MS}}$ factorization and renormalization scale, and \otimes stands for the Mellin convolution in the momentum variable. For brevity writing out only the flavor-singlet case, \mathbf{q}^γ is given by

$$\mathbf{q}^\gamma = \begin{pmatrix} q_s^\gamma \\ g^\gamma \end{pmatrix}, \quad q_s^\gamma \equiv \sum_{j=1}^{n_f} (q_j^\gamma + \bar{q}_j^\gamma) = 2 \sum_{j=1}^{n_f} q_j^\gamma. \quad (2)$$

n_f is the number of active flavors, and the splitting-function matrices are

$$\mathbf{P}^\gamma = \begin{pmatrix} P_{q\gamma} \\ P_{g\gamma} \end{pmatrix}, \quad \mathbf{P} = \begin{pmatrix} P_{qq} & P_{qg} \\ P_{gq} & P_{gg} \end{pmatrix}. \quad (3)$$

The expansions of the photon–parton and parton–parton splitting functions up to NNLO read, with $a_s \equiv \alpha_s/(4\pi)$,

$$\mathbf{P}^\gamma = a_{\text{em}} \left(\mathbf{P}_\gamma^{(0)} + a_s \mathbf{P}_\gamma^{(1)} + a_s^2 \mathbf{P}_\gamma^{(2)} \right), \quad (4)$$

$$\mathbf{P} = a_s \mathbf{P}^{(0)} + a_s^2 \mathbf{P}^{(1)} + a_s^3 \mathbf{P}^{(2)}. \quad (5)$$

The hadronic quantities $\mathbf{P}^{(2)}$ in Eq. (5) can be found in Refs. [8,9]. Our new results for the photonic non-singlet (see Ref. [7] for notational details) and gluon $\overline{\text{MS}}$ splitting functions $\mathbf{P}_\gamma^{(2)}$ in Eq. (4) can be parametrized as

$$\begin{aligned}
\delta_{ns}^{-1} P_{ns\gamma}^{(2)}(x) \cong & 128/27L_1^4 + 112/9L_1^3 + 175.3L_1^2 + 142.3L_1 + 1353 - 1262x \\
& + 449.2x^2 - 1445x^3 - L_0L_1(162.7L_0 + 195.4L_1) + 1169xL_0 \\
& + 50.08(1-x)L_1^3 + 744.6L_0 + 201.6L_0^2 + 80/3L_0^3 + 64/27L_0^4 \\
& + n_f\{-32/27L_1^3 - 11.858L_1^2 - 18.77L_1 - 40.035 + 114.4x \\
& - 24.86x^2 - 53.39x^3 + L_0L_1(8.523L_0 + 269.4L_1) - 26.63xL_0 \\
& + 270.0(1-x)L_1^2 - 21.55L_0 - 10.992L_0^2 - 32/27L_0^3\} \quad (6)
\end{aligned}$$

and

$$\begin{aligned}
\delta_s^{-1} P_{g\gamma}^{(2)}(x) \cong & (1-x)\{32/27L_1^3 - 79.13L_1^2 + 87.22L_1 + 1738 - 1580x \\
& - 160.0x^2 - 566.7x^3 - L_0L_1(549.5 + 1230L_0 + 433.2L_1) \\
& + 2176L_0 + 1123.7L_0^2 + 2400/27L_0^3 + 448/27L_0^4 - 73.1409x^{-1} \\
& + 128/3x^{-1}L_0\} + n_f(1-x)\{-32/9L_1^2 + 16.38L_1 + 68.10 \\
& - 36.42x + 56.95x^2 - 44.10x^3 - L_0L_1(16.18 + 38.33L_0 \\
& + 9.133L_1) - 10.76L_0 + 26.41L_0^2 - 64/27L_0^3 - 40.5597x^{-1}\} \quad (7)
\end{aligned}$$

with $L_0 \equiv \ln x$ and $L_1 \equiv \ln(1-x)$. These parametrizations deviate from the lengthy full expressions by about 0.1% or less, an accuracy which should be amply sufficient for practical applications. On the other hand, the exact expression is very compact for the NNLO pure-singlet splitting function

$$\begin{aligned}
\delta_s^{-1} P_{ps\gamma}^{(2)}(x) = & 4/3n_f\{2464/81x^{-1} - 432 - 72x + 38360/81x^2 \\
& - L_0(344 + 368x + 3584/27x^2) - L_0^2(144 + 104x + 224/9x^2) \\
& - L_0^3(16 - 16x - 128/9x^2) - L_0^4 8/3(1-2x)\}. \quad (8)
\end{aligned}$$

Recall that $P_{q\gamma}$ in Eqs. (3) and (4) is given by $P_{q\gamma} = \delta_s/\delta_{ns} P_{ns\gamma} + P_{ps\gamma}$ with $\delta_s = 3 \sum_{j=1}^{n_f} e_{qj}^2$. A pure-singlet term enters at order $\alpha\alpha_s^2$ for the first time.

Our complete results for $P_{p\gamma}^{(2)}$, $p = q, g$, are compared in Fig. 1 with the previous approximations of Ref. [7]. In Fig. 2 these results are combined, after transformation to the DIS $_{\gamma}$ scheme [6, 7], with the lower-order splitting functions. As indicated by the previous approximate results, the perturbative expansion is well-behaved at least at $x \gtrsim 0.1$. For a further discussion, including the small- x limit, the reader is referred to Ref. [11].

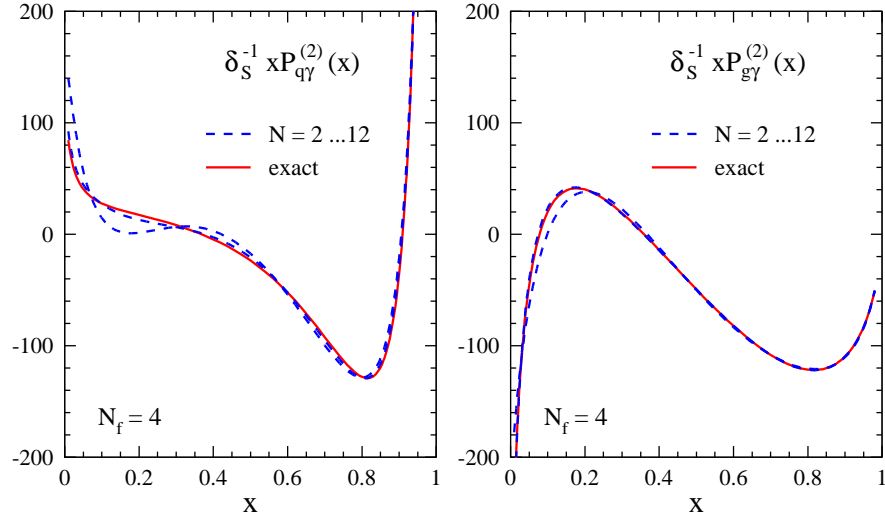


Fig. 1. The exact results for the $a_{\text{em}} a_s^2$ photon-quark (left) and photon-gluon (right) splitting functions (multiplied by x) in the $\overline{\text{MS}}$ scheme, compared with the (dashed) estimated error bands based on the lowest six even-integer moments [7].

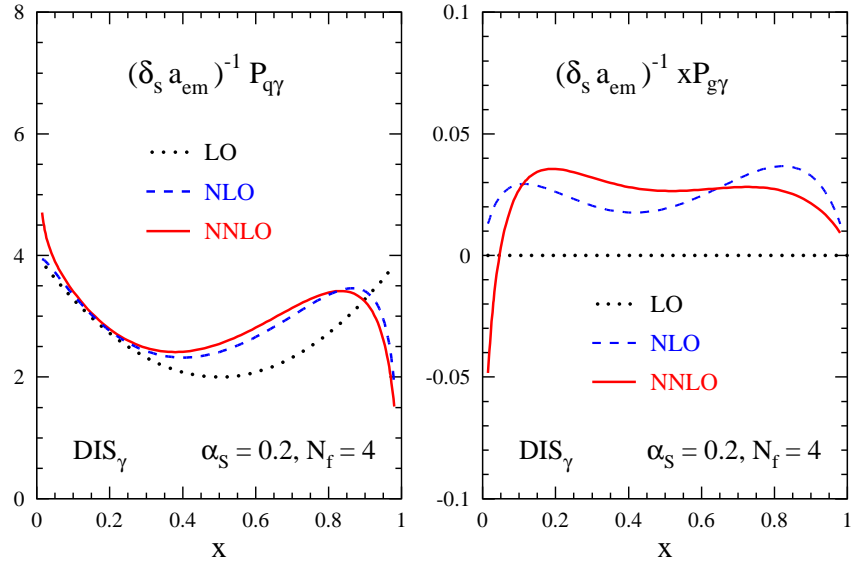


Fig. 2. The perturbative expansion (4) of the photon-quark (left) and photon-gluon (right, multiplied by x) splitting functions in the DIS_γ factorization scheme for typical values of α_s and n_f . Note the very different scales of the two graphs.

REFERENCES

- [1] E. Witten, *Nucl. Phys.* **B120**, 189 (1977).
- [2] W.A. Bardeen, A. Buras, *Phys. Rev.* **D20**, 166 (1979); **D21**, 2041 (1980) (E).
- [3] R.J. De Witt *et al.*, *Phys. Rev.* **D19**, 2046 (1979); **D20**, 1751 (1979) (E).
- [4] M. Glück, E. Reya, *Phys. Rev.* **D28**, 2749 (1983).
- [5] M. Fontannaz, E. Pilon, *Phys. Rev.* **D45**, 382 (1992); **D46**, 484 (1992) (E).
- [6] M. Glück, E. Reya, A. Vogt, *Phys. Rev.* **D45**, 3986 (1992).
- [7] S. Moch, J.A.M. Vermaseren, A. Vogt, *Nucl. Phys.* **B621**, 413 (2002).
- [8] S. Moch, J.A.M. Vermaseren, A. Vogt, *Nucl. Phys.* **B688**, 101 (2004).
- [9] A. Vogt, S. Moch, J.A.M. Vermaseren, *Nucl. Phys.* **B691**, 129 (2004).
- [10] J.A.M. Vermaseren, A. Vogt, S. Moch, *Nucl. Phys.* **B724**, 3 (2005).
- [11] S. Moch, J.A.M. Vermaseren, A. Vogt, in preparation.